



# Topical Antibiotic Elution in a Collagen-Rich Hydrogel Successfully Inhibits Bacterial Growth and Biofilm Formation *In Vitro*

Jung Gi Min,<sup>a,b</sup> Uriel J. Sanchez Rangel,<sup>a,b</sup> Austin Franklin,<sup>a,b</sup> Hiroki Oda,<sup>a,b</sup> Zhen Wang,<sup>a,b</sup> James Chang,<sup>a,b</sup>  Paige M. Fox<sup>a,b</sup>

<sup>a</sup>Division of Plastic & Reconstructive Surgery, Department of Surgery, Stanford University School of Medicine, Stanford, California, USA

<sup>b</sup>Division of Plastic & Reconstructive Surgery, Veterans Affairs Palo Alto Health Care System, Palo Alto, California, USA

**ABSTRACT** Chronic wounds are a prominent concern, accounting for \$25 billion of health care costs annually. Biofilms have been implicated in delayed wound closure, but they are susceptible to developing antibiotic resistance and treatment options continue to be limited. A novel collagen-rich hydrogel derived from human extracellular matrix presents an avenue for treating chronic wounds by providing appropriate extracellular proteins for healing and promoting neo-vascularization. Using the hydrogel as a delivery system for localized secretion of a therapeutic dosage of antibiotics presents an attractive means of maximizing delivery while minimizing systemic side effects. We hypothesize that the hydrogel can provide controlled elution of antibiotics leading to inhibition of bacterial growth and disruption of biofilm formation. The rate of antibiotic elution from the collagen-rich hydrogel and the efficacy of biofilm disruption was assessed with *Pseudomonas aeruginosa*. Bacterial growth inhibition, biofilm disruption, and mammalian cell cytotoxicity were quantified using *in vitro* models. The antibiotic-loaded hydrogel showed sustained release of antibiotics for up to 24 h at therapeutic levels. The treatment inhibited bacterial growth and disrupted biofilm formation at multiple time points. The hydrogel was capable of accommodating various classes of antibiotics and did not result in cytotoxicity in mammalian fibroblasts or adipose stem cells. The antibiotic-loaded collagen-rich hydrogel is capable of controlled antibiotic release effective for bacteria cell death without native cell death. A human-derived hydrogel that is capable of eluting therapeutic levels of antibiotic is an exciting prospect in the field of chronic wound healing.

**KEYWORDS** antibiotic elution, biofilm, collagen-rich hydrogel, topical antibiotics

Chronic wounds are a serious concern in the face of rising rates of obesity, peripheral vascular disease, and diabetes, costing the health care system \$25 billion a year (1). Pressing issues in chronic wound care include bacterial wound colonization, infections, and biofilm formation. Biofilms are implicated in delayed wound closure due to impaired immune responses and delayed epithelization (2–4). Biofilms are difficult to treat due to cell-cell interactions and resistance to systemic antibiotic treatment, sometimes requiring 10 to 1,000 times the antibiotic concentration (5–8). Resistance to antibiotics is conferred through multiple mechanisms, including decreased drug penetration, formation of nutrient gradients, development of a highly protected persister state, and horizontal transfer of resistant genes. Furthermore, blood flow is often limited in chronic wounds, making systemic antibiotic treatment less effective due to poor bioavailability (9). Therefore, treatment for chronic wound infections must be aggressive with high dosages of systemic antibiotics that remain safe for renal and hepatic function (10).

**Citation** Min JG, Sanchez Rangel UJ, Franklin A, Oda H, Wang Z, Chang J, Fox PM. 2020. Topical antibiotic elution in a collagen-rich hydrogel successfully inhibits bacterial growth and biofilm formation *in vitro*. *Antimicrob Agents Chemother* 64:e00136-20. <https://doi.org/10.1128/AAC.00136-20>.

This is a work of the U.S. Government and is not subject to copyright protection in the United States. Foreign copyrights may apply. Address correspondence to Paige M. Fox, [pfox@stanford.edu](mailto:pfox@stanford.edu).

**Received** 21 January 2020

**Returned for modification** 24 February 2020

**Accepted** 1 July 2020

**Accepted manuscript posted online** 20 July 2020

**Published** 21 September 2020

Localized release of therapeutic concentrations of antibiotics presents an attractive treatment option in this resistant population. This system maximizes local delivery while minimizing systemic side effects (11, 12). Local antibiotic carriers have been shown to elute 10 to 100× the MIC while limiting serum concentrations (13). Less systemic effects lead to increased compliance and a decreased need for follow-up (14). Localized delivery is also pertinent in the context of antibiotic stewardship. Controlled release at higher doses can prevent subtherapeutic concentrations of antibiotic from breeding resistant strains (12, 15, 16).

Hydrogel, a three-dimensional polymeric network, is an intriguing vehicle for sustained antibiotic delivery to wounds due to its stable architecture and its potential to carry various compounds (17, 18). Antimicrobial agents typically suffer from proteolytic instability, but the conjugation of antibiotic to the polymer hydrogel can lead to prolonged antimicrobial efficacy (19). Most examples of antibiotic-impregnated hydrogels have been in orthopedic surgery in the treatment of osteomyelitis, but there has been a recent explosion across multiple applications such as wound healing (6, 20). Previous examples include loaded hydrogels with metallic nanoparticles (21, 22), inherently antimicrobial hydrogels (23), and other antimicrobial agents (24–26). Although there are many studies utilizing the hydrogel as a vehicle for antibiotic delivery in acute wounds, applications in chronic wounds and biofilms have not yet been thoroughly studied.

A novel collagen-rich hydrogel (cHG) derived from human extracellular matrix presents an exciting avenue for treating chronic wounds. This scaffold has been described extensively in previous studies (27). The gel is unique in its derivation from human tissue, thereby providing the wound with an appropriate milieu of proteins that can be utilized as building blocks for wound healing. The derivation of the hydrogel is straightforward and does not require complex machinery, facilitating translation to clinical use. The composition from native proteins results in biocompatibility that minimizes immune response compared to that with animal-derived or recombinant proteins that have been reported to have decreased bioactivity and increased immunogenicity (28, 29). The gel also contains native signaling molecules that increase neovascularization. This gel has already been shown to accelerate healing on its own in a previous study with a diabetic wound model (30). This combination of favorable characteristics makes the cHG an intriguing treatment option in the paradigm of local antibiotic delivery.

This study examines the capacity of the cHG to act as a vehicle for antibiotic elution. We hypothesize that this hydrogel can control the release of antibiotics for an extended duration and subsequently disrupt biofilms, augmenting its previously observed healing effects. Here, we examined the elution profiles of antibiotics from the hydrogel. We then use established models *in vitro* to evaluate the effect of cHG-antibiotic treatment on biofilms formed by *Pseudomonas aeruginosa*, a major organism implicated in chronic wounds.

(This work was presented at Stanford Plastic Surgery Research Symposium 2019 and Holman Research Day 2019, Stanford, CA.)

## RESULTS

**Rate of gentamicin elution.** The concentration of gentamicin eluted from the cHG-antibiotic composite (cHG-abx) was compared to a gentamicin solution control over various time points as shown in Fig. 1. The control showed consistent concentration of eluted gentamicin, as expected. The elution curve demonstrated 50% gentamicin elution within the first 6 to 12 h. The maximum concentration of gentamicin was achieved in 2 days.

**Inhibition of bacterial growth.** A modified Kirby-Bauer assay showed retained inhibitory effects of cHG-abx after 48 h of preelution (Fig. 2). The zone of inhibition in the composite applied immediately after mixing cHG and antibiotic was  $1.04 \pm 0.09$  cm<sup>2</sup>. The zone decreased to  $0.51 \pm 0.13$  cm<sup>2</sup> in the group with 48 h of preelution. Overall, the magnitude of inhibition decreased as the duration of preelution increased.

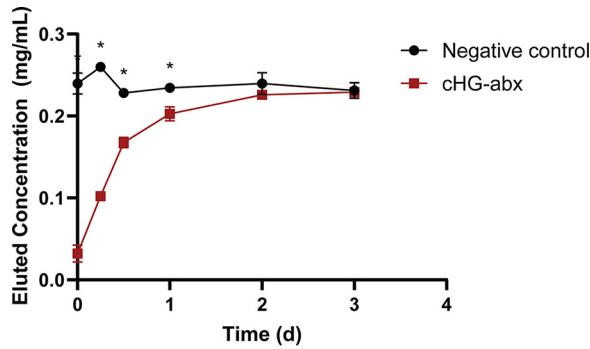


**FIG 1** Rate of antibiotic elution. The concentration of gentamicin eluted from cHG is represented as a function of time, compared between control (gentamicin solution) and treatment (cHG-abx). Each experiment was performed in triplicates. \*,  $P < 0.05$  versus control.

**Disruption of biofilm.** The disruptive effects of the cHG-abx on biofilms were studied in three different models. The polycarbonate membrane model showed a significantly lower bacterial count in treatment groups for up to 24 h of preelution (Fig. 3A). At 24 h, there was a 35.2% decrease in bacteria compared to that in the control. The treatment group with 48 and 72 h of preelution did not show a statistically significant decrease in bacterial count.

The crystal violet assay was used to examine biofilm disruption on a tissue culture plate. The crystal violet staining, indicating the strength of the biofilm, was significantly decreased with cHG-abx treatment (Fig. 3B). This effect is less pronounced but remained in the treatment group that was preeluted for 24 h.

The disruption of biofilm as visualized on a polycarbonate membrane through the SYTO 61 nucleic acid label is shown in Fig. 3C. The assay qualitatively showed less bacteria in the treatment groups than in the control group in the central part of the membrane. In the group with 24 h of preelution, faint traces of the bacterial biofilm remained visible.

Biofilm disruption by different compositions of cHG-abx is shown in Fig. 4. The polycarbonate model was used as described above. cHG-abx formed from gentamicin, ceftazidime, and ciprofloxacin all demonstrated significantly reduced bacterial counts compared to that of the control. This effect was maintained for 24 h in all 3 groups and for 48 h in the ciprofloxacin group.

**Cytotoxicity on mammalian cells.** The possible cytotoxic effect of the cHG-abx on mammalian cells was visualized through the LIVE/DEAD assay (Fig. 5). There was no measurable difference between live cells (fibroblasts [FB] or adipose-derived stem cells [ASC]) in the treatment group versus that in the control. Cellular densities of ASC and fibroblasts also remained relatively consistent at 24 h of incubation (see Fig. S1 in the supplemental material).

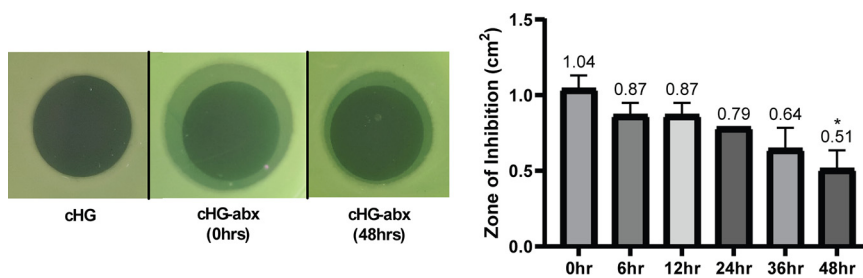


**FIG 2** Modified Kirby-Bauer assay. The zones of inhibition (ZOIs) between cHG-abxs allowed to preelute for variable durations (represented in hours) were compared. Representative images (left) and comparisons between various time points (right) are shown. Each experiment was performed in duplicates. \*,  $P < 0.1$  versus control. Numbers above the bars represent the averages.

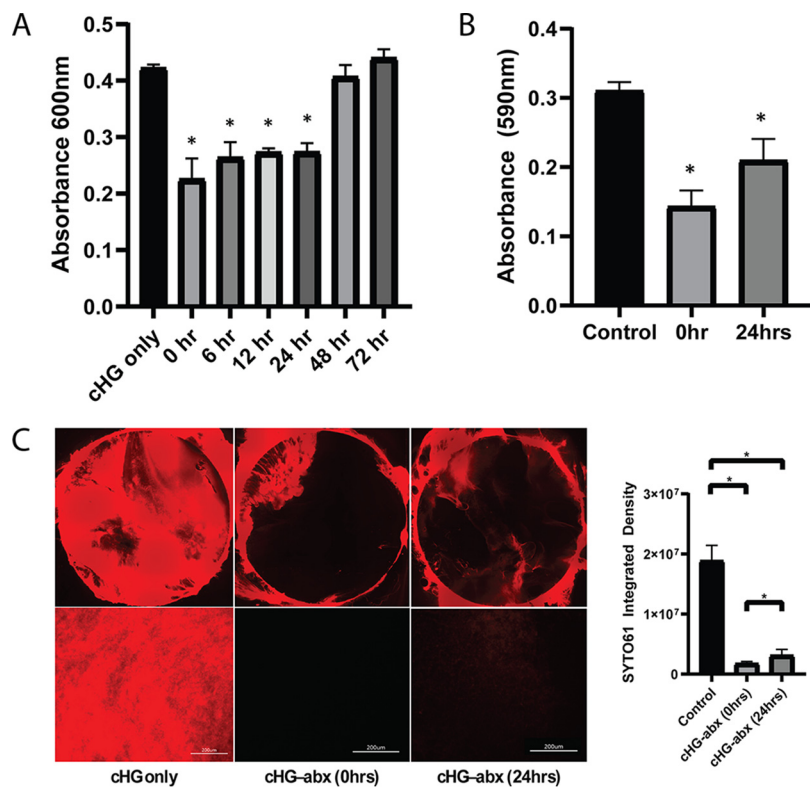


**FIG 3** Disruption of biofilm. Biofilm disruption was evaluated using 3 different models. Time points (hours) on the x axis represent the amount of time the composite was preeluted before treatment. (A) Polycarbonate membrane model: the bacterial count in the biofilm after treatment is represented as an  $A_{600}$ . \*,  $P < 0.05$  versus control. (B) Crystal violet assay: crystal violet staining of biofilm in a 12-well plate is represented as  $A_{590}$ . \*,  $P < 0.05$  versus control. (C) SYTO 61 imaging: visualization by SYTO 61 nucleic acid stain. The red represents live bacteria. The image of the entire biofilm membrane is shown (top) as well as representative images at higher magnification (bottom). \*,  $P < 0.05$ .

**DISCUSSION**

Human-derived collagen-rich hydrogel is capable of releasing therapeutic levels of antibiotics for 24 h, leading to an inhibition of bacterial growth and disruption of bacterial biofilms. As expected, the magnitude of the effect decreases over time but remains effective after 1 day of preelution.

Furthermore, we have demonstrated that cHG is compatible with various classes and concentrations of antibiotics. This has significant implications, making it possible to

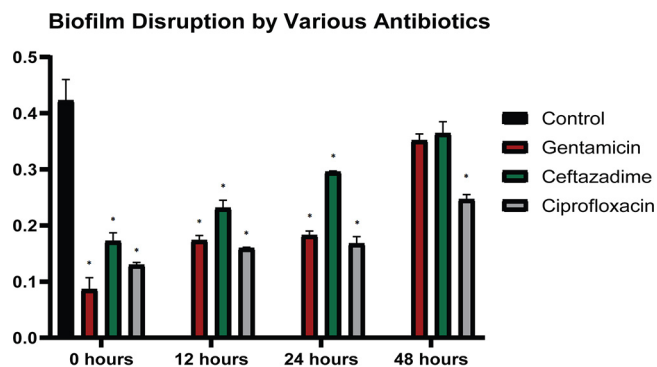


**FIG 4** cHG composites with other antibiotics. The biofilm disruption by various antibiotics eluted from the cHG is represented. Bacterial quantification as absorbance at 600 nm is compared across different types of antibiotics. The duration (in hours) on the x axis represents the time of preelution of the cHG-abx before treatment. \*,  $P < 0.05$  versus control.

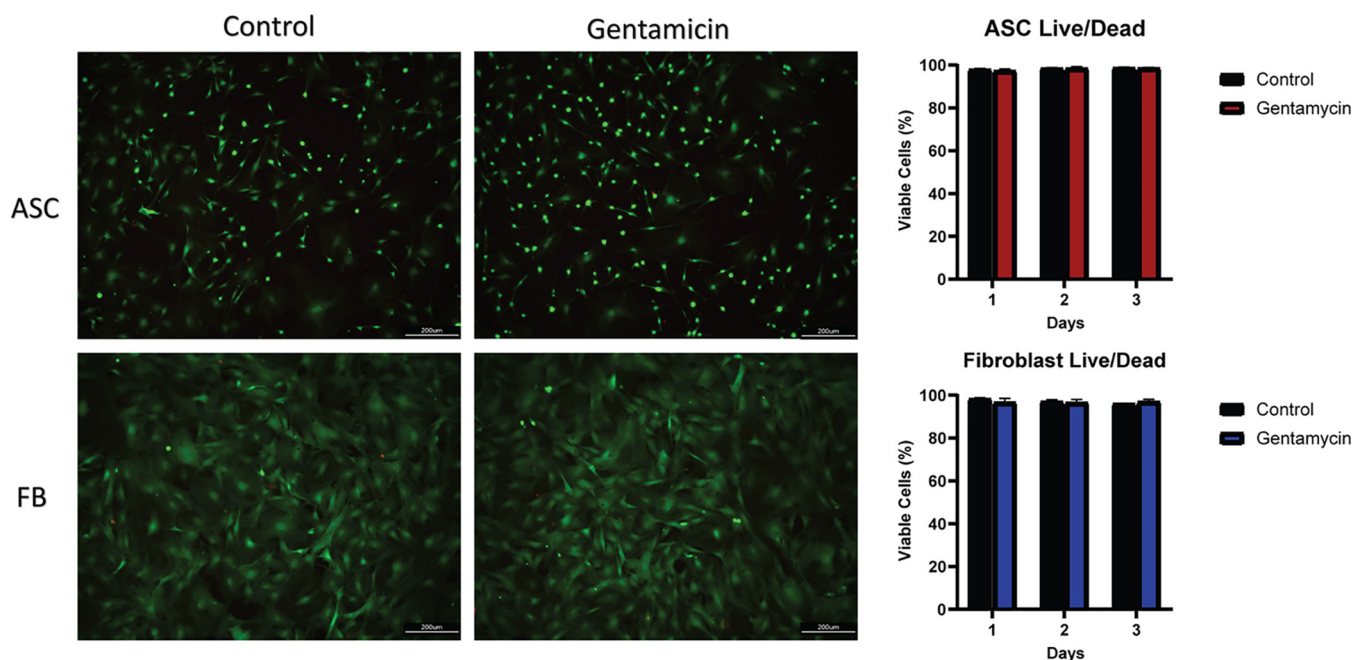


**FIG 5** Cytotoxicity in mammalian cells. The cytotoxicity of the cHG-abx hydrogel on adipose stem cells (ASC) and fibroblasts (FB) is represented in the LIVE/DEAD assay. In both the control and gentamicin groups, green represents live cells, and red represents dead cells (left). Viable cells as percentages in different cell lines and treatment groups is also shown (right).

customize the antibiotic treatment to the individual patient depending on the patient's specific bacteria and their antimicrobial sensitivity profile. Currently, many antimicrobial dressings on the market contain nonspecific agents such as silver and iodine (31), whose effectiveness is not supported by rigorous data and may be effective for certain bacteria but not others (32).

We observed no toxicity of the composite on mammalian ASCs and fibroblasts, indicating that the combination of antibiotics and cHG is safe for local administration. The remarkable biocompatibility of collagen gels has been reported previously, which corroborate our results (33). This is an important benefit of using native polymer hydrogels as opposed to synthetic fabrications. Despite the control over physical and chemical properties that can be gained, synthetic hydrogels tend to be less biocompatible and bioactive (34).

The potential application to the clinical setting is intriguing. The dual function of providing key extracellular proteins for wound healing and acting as a carrier for antibiotic release addresses the two key issues faced in chronic wound treatment. From previously published studies, we have seen that the hydrogel itself has healing properties (35, 36). It provides collagen, known to be a powerful agent to stimulate healing (27). Our hydrogel, furthermore, contains signaling molecules and cues for increased vascularization (30). It is also biodegradable and biocompatible, as seen *in vivo* models (36). These powerful wound healing effects can be augmented by the addition of antibiotics to the composite formulation to combat wound infection.

Additionally, efficient and effective antibiotic delivery is crucial in the context of antibiotic stewardship. According to the CDC, "antibiotic resistance is one of the most urgent threats to the public's health" (37). Decreased drug delivery to chronic wounds due to reduced vascularization leads to subtherapeutic concentration of antibiotics locally. Additionally, biofilm formation lowers the concentration of antibiotic to which the bacteria are exposed. Both of these factors lead to the breeding of resistant strains of bacteria. Indeed, there has been an increase in antibiotic-resistant bacterial strains associated with chronic wounds (38). The cHG-abx used here is an option to combat this risk for antibiotic resistance by delivering a high local concentration of antibiotics



to the wound. Furthermore, the composite can be customized with multiple narrow-spectrum antibiotics to reduce the need for broad-spectrum antibiotics, whose usage can also lead to increased resistance to common antibiotics.

One major limitation of collagen-based hydrogels in antibiotic delivery has been the rate of release. Studies have shown that fibrillar collagen gels without any modifications release small drugs within minutes (39). The cHG from this study elutes antibiotics for a longer duration of 2 days. It is possible that the fact our hydrogel is composed of other proteins than collagen could contribute to slower release. The intended application of the cHG-abx studied here is for chronic wound healing where dressings are often changed daily or multiple times per day (40). Additionally, in previous studies in our lab examining cHG alone for wound healing *in vivo*, cHG was changed every other day and demonstrated superior wound healing to that of the control in a stented diabetic wound model (30). The pharmacodynamics of the eluted antibiotics from topical application was not studied in this *in vitro* study. Future *in vivo* studies will examine circulating antibiotic levels and potential nephrotoxicity and hepatotoxicity. Other studies have attempted to use various scaffolds to deliver antibiotics to wounds. A major class of carrier systems is polymethylmethacrylate (PMMA) beads, which can provide structure and elute antibiotics for weeks to even years (6). A drawback to PMMA beads is that they are not biodegradable and require surgical extraction to avoid biofilm development. Another interesting possibility is designing inherently antimicrobial hydrogels using polycationic material to disrupt membranes (23). More recently, there has been a growing interest in incorporating antibiotic-impregnated nanoparticles to organic hydrogels. Despite promising results, the use of this composite for treatment is still incomplete, and knowledge of the interaction with cells and tissues as well as nanotoxicology and safety are lacking (41). Future studies will be needed to compare the healing potential of cHG with other scaffolds currently being developed.

One limitation of this study is that only one strain of bacteria was studied. *Pseudomonas aeruginosa* is a major biofilm producer complicating chronic wounds, but there are others, including *Staphylococcus*, *Enterococcus*, and *Enterobacter*, each with distinct patterns for biofilm formation (42). In fact, most natural biofilms consist of multiple strains of bacteria, creating an entire ecosystem (43). Initial experiments from our group using the *Escherichia coli* K-12 species have been promising, demonstrating similar patterns as described in this study (see Fig. S2 in the supplemental material). Follow-up studies of other strains and species of biofilm-producing bacteria are needed, both individually and in combination to expand the potential impact of cHG-abx.

Limitations of using *in vitro* models to study biofilm physiology have been discussed previously (44). The microenvironment of biofilm is complex, and the exact composition of the exopolysaccharide (EPS) can change based on the composition of the growing surface, especially in biofilms produced by *P. aeruginosa*. In the present study, multiple *in vitro* models supported by previous literature were utilized that employed different growing surfaces such as agar gels, polycarbonate discs, and cell culture plates. Ultimately, it will be important to continue this work with *in vivo* models that may more accurately replicate the microenvironment of the biofilm.

We have demonstrated that a novel human-derived collagen-rich hydrogel is an effective vehicle for controlled release of antibiotics without associated mammalian cytotoxicity. Additionally, the antibiotics released by cHG inhibited bacterial growth and disrupted biofilm formation. A human-derived hydrogel possessing essential proteins for wound healing that is capable of eluting therapeutic levels of antibiotic is an exciting prospect in the field of chronic wound healing. Future directions will utilize established chronic wound models in diabetic mice to examine the effects of cHG-abxs on biofilm production and overall wound progression.

## MATERIALS AND METHODS

**Collagen hydrogel formation.** Three percent collagen-rich thermoresponsive hydrogel (cHG) was synthesized according to prior established protocols (27). Briefly, flexor tendons were harvested from

fresh cadaveric donors of mixed sex and age (>18 years). These were decellularized, lyophilized, and ground into powder. Samples were digested with 1 mg/ml of pepsin (Sigma-Aldrich, St. Louis, MO) at pH 2.2. After 14 h of digestion, the reaction was stopped and the pH adjusted to 7.4. The quality of the gel was confirmed microscopically, and gelation was confirmed following incubation at 37°C.

**Rate of gentamicin elution from cHG.** Hydrogel in its liquid form was mixed with stock gentamicin solution (Acros Organics, Fair Lawn, NJ) of concentration 10 mg/ml. This concentration corresponds linearly with the absorption of ninhydrin in the colorimetric assay described below. Subsequently, 300  $\mu$ l of the hydrogel-gentamicin composite (experimental group) or gentamicin solution in phosphate-buffered saline (PBS; control) was pipetted into the bottom of a sterile 5-ml tube, and the tube incubated in 37°C for 1 h for gelation/incubation. Four milliliters of PBS was added to the top of the hydrogel, and the tube was incubated in a water bath at 37°C. The PBS solution was sampled periodically at set time points (0, 6, 12, 24, 48, and 72 h), and the volume sampled was replaced with fresh PBS. Eluted samples were immediately frozen at -20°C, and all samples were analyzed at the same time.

Concentrations of gentamicin in the eluted samples were analyzed through the ninhydrin colorimetric assay, which has been proved to be a reproducible, efficient, and safe method of detecting concentrations of gentamicin (45, 46). Briefly, 5 mg/ml ninhydrin stock solution was formed by dissolving ninhydrin powder (VWR International, Radnor, PA) in PBS. Elution samples were mixed with the stock ninhydrin solution at a 1:1 ratio. The solution was put on a heat block at 95°C for 15 min, followed by incubation in an ice bath for 10 min. The solution was evaluated by spectrophotometry at a wavelength of 418 nm. Each experiment was performed in triplicates.

**cHG-antibiotic composite preparation.** Gentamicin sulfate (Thermo Fischer Scientific, Waltham, MA), ceftazidime pentahydrate (Thermo Fischer Scientific), and ciprofloxacin (Thermo Fischer Scientific) were dissolved according to the manufacturer's instructions to form a stock solution. These antibiotics were chosen based on the antibiotic sensitivity profile and clinical relevance. Stock solutions were mixed with the cHG in its liquid form, and 10  $\mu$ l of the composite was pipetted onto polycarbonate filter membranes. The final amounts of antibiotic delivered for gentamicin (1 mg), ceftazidime (0.5 mg), and ciprofloxacin (2 mg) were calculated as 10 to 100 $\times$  MIC in a theoretical 1-ml space as described for *Pseudomonas aeruginosa* by the Clinical and Laboratory Standards Institute (CLSI) (47). The composites on polycarbonate membranes were incubated at 37°C for 1 h to ensure gelation. The composites were then covered with PBS and allowed to incubate until predetermined time points. The start times for the formation of the composites were staggered so that treatment groups of various preelution durations could be compared at the same time.

**Bacterial strain and growth conditions.** *Pseudomonas aeruginosa* (ATCC 27853) was used in all experiments. *P. aeruginosa* was grown in Luria Bertani (LB) broth at 37°C overnight. Bacterial cultures were used at mid-log growth phase, between 0.2 and 0.3 by absorbance at 600 nm.

**Modified Kirby-Bauer assay.** The efficacy of the cHG-antibiotic composite (cHG-abx) in inhibiting bacterial growth was studied through a modified Kirby-Bauer disk diffusion assay using established protocols (48). Two hundred microliters of 10<sup>8</sup> CFU/ml *P. aeruginosa* was seeded onto a Mueller-Hinton agar plate and allowed to incubate for 30 min. cHG-gentamicin composites preeluted for different amounts of time were added to the top of the agar plate. The plates were then incubated at 37°C for 16 h. The zone of inhibition (ZOI) was measured from the center of the composite to the zone perimeter, and the total area of the zone was calculated. Images were taken of the observed inhibition.

**Biofilm disruption.** Biofilm disruption was assessed using three biofilm models outlined below.

**(i) Polycarbonate biofilm model.** Biofilms were prepared according to the method developed by the Center for Biofilm Engineering at Montana State University (49). Briefly, 1.3-cm-diameter polycarbonate membrane filters (0.2- $\mu$ m pore size) (Millipore Sigma, Hayward, CA) were sterilized with UV light for 10 min on both sides. *P. aeruginosa* was grown to approximately 10<sup>8</sup> CFU/ml and diluted 1:100 in LB broth. Two microliters of solution was placed on each filter, and the filter was plated onto LB plates cultured at 37°C for 24 h. The incubated biofilms were transferred to fresh LB plates. cHG-abxs preeluted in PBS for various time points as outlined above were added on top of the biofilm as treatment. cHG without antibiotics was used as a control. Plates were incubated at 37°C for 12 to 16 h.

Treated biofilms were then analyzed. The biofilm was added to a conical vial with 9.0 ml PBS. The mixture was vortexed at high speed for 2.0 min. Spectrometry was used to measure the absorbance of the resulting mixture at 600 nm. Samples of the solution were serially diluted and seeded onto plates to ensure correlation between colony counts of bacteria and absorbance of light at 600 nm.

**(ii) Crystal violet assay.** Biofilm disruption was studied using a modified crystal violet (CV) assay described previously (50). Bacterial suspension in LB broth as described above was incubated in 12-well tissue culture-treated plates (1 ml per well). After 24 h of growth and formation of biofilm, cHG-abxs with different durations of preelution in PBS were added to the top of the formed biofilm and incubated for 12 to 16 h. After incubation, wells were emptied and washed 3 times in distilled water (dH<sub>2</sub>O). One milliliter of 0.3% solution of crystal violet was added to each well, and the plate was incubated for 20 min. The CV solution was removed, and wells were washed 3 times more. After drying for 1 h, 1 ml of 95% ethanol was added to dissolve the CV, and absorbance was quantified in a plate reader at 595 nm.

**(iii) Fluorometric visualization.** Bacterial suspension in LB broth as described above was incubated in 12-well tissue culture-treated plates. A polycarbonate membrane filter was placed in each well and incubated for 24 h. cHG-abxs were added to each well, on top of the polycarbonate membrane filter, and incubated for 12 to 16 h. After incubation, the biofilm membrane was removed and washed in dH<sub>2</sub>O and placed in a fresh well. A 1-ml aliquot of the nucleic acid stain SYTO 61 (Invitrogen, Carlsbad, CA) was diluted 1:100 in PBS and added to each well. The plates were incubated for 30 min at room temperature. The membranes were then removed from the solution and rinsed with sterile dH<sub>2</sub>O. The membranes

were placed onto a glass slide and covered with a glass coverslip. Visualization of the biofilms formed on the polycarbonate membranes were visualized with a KEYENCE fluorescence microscope (BZ-X700; KEYENCE, Osaka, Japan). Images of the polycarbonate membrane and representative images at higher magnification were taken.

**Mammalian cell cytotoxicity.** Adipose-derived stem cells (ASCs) and fibroblasts (FB) (Cell Applications, San Diego, CA) were grown to 95% confluence in a humidifier in cell-specific growth media. These cell lines were chosen to study cytotoxicity in both differentiated and undifferentiated mammalian cells. Cells were lifted and seeded onto 24-well culture plates at  $2 \times 10^4$  cells/ml and allowed to attach overnight. cHG-abx treatments were added to the wells with the cells and allowed to incubate until predetermined time points.

A LIVE/DEAD viability/cytotoxicity assay (Thermo Fischer Scientific) was used according to the manufacturer's instructions. After removal of cell culture media from the wells, LIVE/DEAD reagent was added and incubated at 37°C for 30 min. The cells were visualized using the KEYENCE fluorescence microscope (KEYENCE BZ-X700). The resulting images were analyzed using Image J software (NIH, Bethesda, MD). All experiments were performed in triplicates.

**Statistical analysis.** Results are reported in the respective units  $\pm$  standard deviation (SD), and the differences were evaluated relative to the control with an unpaired *t* test. Significance was set to a *P* value of  $<0.05$ .

## SUPPLEMENTAL MATERIAL

Supplemental material is available online only.

**SUPPLEMENTAL FILE 1**, PDF file, 0.5 MB.

## ACKNOWLEDGMENT

We have no financial interest in any of the organizations discussed in this paper.

## REFERENCES

- Zhao G, Usui ML, Lippman SI, James GA, Stewart PS, Fleckman P, Olerud JE. 2013. Biofilms and inflammation in chronic wounds. *Adv Wound Care (New Rochelle)* 2:389–399. <https://doi.org/10.1089/wound.2012.0381>.
- Fazli M, Bjarnsholt T, Kirketerp-Møller K, Jørgensen A, Andersen CB, Givskov M, Tolker-Nielsen T. 2011. Quantitative analysis of the cellular inflammatory response against biofilm bacteria in chronic wounds. *Wound Repair Regen* 19:387–391. <https://doi.org/10.1111/j.1524-475X.2011.00681.x>.
- Seth AK, Geringer MR, Gurjala AN, Hong SJ, Galiano RD, Leung KP, Mustoe TA. 2012. Treatment of *Pseudomonas aeruginosa* biofilm-infected wounds with clinical wound care strategies: a quantitative study using an *in vivo* rabbit ear model. *Plast Reconstr Surg* 129:262e–274e. <https://doi.org/10.1097/PRS.0b013e31823aeb3b>.
- James GA, Swogger E, Wolcott R, Pulcini ED, Secor P, Sestrich J, Costerton JW, Stewart PS. 2008. Biofilms in chronic wounds. *Wound Repair and Regeneration* 16:37–44. <https://doi.org/10.1111/j.1524-475X.2007.00321.x>.
- Wolcott R, Rhoads D, Bennett M, Wolcott B, Gogokhia L, Costerton J, Dowd S. 2010. Chronic wounds and the medical biofilm paradigm. *J Wound Care* 19:45–53. <https://doi.org/10.12968/jowc.2010.19.2.46966>.
- Markakis K, Faris AR, Sharaf H, Faris B, Rees S, Bowling FL. 2018. Local antibiotic delivery systems: current and future applications for diabetic foot infections. *Int J Low Extrem Wounds* 17:14–21. <https://doi.org/10.1177/1534734618757532>.
- Høiby N, Ciofu O, Johansen HK, Song Z, Moser C, Jensen PØ, Molin S, Givskov M, Tolker-Nielsen T, Bjarnsholt T. 2011. The clinical impact of bacterial biofilms. *Int J Oral Sci* 3:55–65. <https://doi.org/10.4248/IJOS11026>.
- Hengzhuang W, Wu H, Ciofu O, Song Z, Høiby N. 2011. Pharmacokinetics/pharmacodynamics of colistin and imipenem on mucoid and nonmucoid *Pseudomonas aeruginosa* biofilms. *Antimicrob Agents Chemother* 55:4469–4474. <https://doi.org/10.1128/AAC.00126-11>.
- Morley R, Lopez F, Webb F. 2016. Calcium sulphate as a drug delivery system in a deep diabetic foot infection. *Foot (Edinb)* 27:36–40. <https://doi.org/10.1016/j.foot.2015.07.002>.
- Wu H, Moser C, Wang H-Z, Høiby N, Song Z-J. 2015. Strategies for combating bacterial biofilm infections. *Int J Oral Sci* 7:1–7. <https://doi.org/10.1038/ijos.2014.65>.
- Peng K-T, Chen C-F, Chu I-M, Li Y-M, Hsu W-H, Hsu R-W, Chang P-J. 2010. Treatment of osteomyelitis with teicoplanin-encapsulated biodegradable thermosensitive hydrogel nanoparticles. *Biomaterials* 31:5227–5236. <https://doi.org/10.1016/j.biomaterials.2010.03.027>.
- Stebbins ND, Ouimet MA, Uhrich KE. 2014. Antibiotic-containing polymers for localized, sustained drug delivery. *Adv Drug Deliv Rev* 78:77–87. <https://doi.org/10.1016/j.addr.2014.04.006>.
- Fleiter N, Walter G, Bösebeck H, Vogt S, Büchner H, Hirschberger W, Hoffmann R. 2014. Clinical use and safety of a novel gentamicin-releasing resorbable bone graft substitute in the treatment of osteomyelitis/osteitis. *Bone Joint Res* 3:223–229. <https://doi.org/10.1302/2046-3758.37.2000301>.
- Kost J, Langer R. 2012. Responsive polymeric delivery systems. *Adv Drug Deliv Rev* 64:327–341. <https://doi.org/10.1016/j.addr.2012.09.014>.
- Yang K, Han Q, Chen B, Zheng Y, Zhang K, Li Q, Wang J. 2018. Antimicrobial hydrogels: promising materials for medical application. *Int J Nanomedicine* 13:2217–2263. <https://doi.org/10.2147/IJN.S154748>.
- Wu P, Grainger DW. 2006. Drug/device combinations for local drug therapies and infection prophylaxis. *Biomaterials* 27:2450–2467. <https://doi.org/10.1016/j.biomaterials.2005.11.031>.
- Hoque J, Bhattacharjee B, Prakash RG, Paramanandham K, Haldar J. 2018. Dual function injectable hydrogel for controlled release of antibiotic and local antibacterial therapy. *Biomacromolecules* 19:267–278. <https://doi.org/10.1021/acs.biomac.7b00979>.
- Li Y, Fukushima K, Coady DJ, Engler AC, Liu S, Huang Y, Cho JS, Guo Y, Miller LS, Tan JPK, Ee PLR, Fan W, Yang YY, Hedrick JL. 2013. Broad-spectrum antimicrobial and biofilm-disrupting hydrogels: stereocomplex-driven supramolecular assemblies. *Angew Chem Int Ed Engl* 52:674–678. <https://doi.org/10.1002/anie.201206053>.
- González-Henríquez C, Sarabia-Vallejos M, Rodríguez-Hernández J. 2017. Advances in the fabrication of antimicrobial hydrogels for biomedical applications. *Materials* 10:232. <https://doi.org/10.3390/ma10030232>.
- Howlin R, Brayford M, Webb J, Cooper J, Aiken S, Stoodley P. 2015. Antibiotic-loaded synthetic calcium sulfate beads for prevention of bacterial colonization and biofilm formation in periprosthetic infections. *Antimicrob Agents Chemother* 59:111–120. <https://doi.org/10.1128/AAC.03676-14>.
- Marsich E, Travan A, Donati I, Di Luca A, Benincasa M, Crosera M, Paoletti S. 2011. Biological response of hydrogels embedding gold nanoparticles. *Colloids Surf B Biointerfaces* 83:331–339. <https://doi.org/10.1016/j.colsurfb.2010.12.002>.
- Zan X, Kozlov M, McCarthy TJ, Su Z. 2010. Covalently attached, silver-doped poly(vinyl alcohol) hydrogel films on poly(L-lactic acid). *Biomacromolecules* 11:1082–1088. <https://doi.org/10.1021/bm100048q>.
- Li P, Poon YF, Li W, Zhu H-Y, Yeap SH, Cao Y, Qi X, Zhou C, Lamrani M, Beuerman RW, Kang E-T, Mu Y, Li CM, Chang MW, Leong SSJ, Chan-Park MB. 2011. A polycationic antimicrobial and biocompatible hydrogel with



- microbe membrane suctioning ability. *Nat Mater* 10:149–156. <https://doi.org/10.1038/nmat2915>.
24. Singh B, Sharma S, Dhiman A. 2013. Design of antibiotic containing hydrogel wound dressings: biomedical properties and histological study of wound healing. *Int J Pharm* 457:82–91. <https://doi.org/10.1016/j.ijpharm.2013.09.028>.
  25. Alvarez GS, Helary C, Mebert AM, Wang X, Coradin T, Desimone MF. 2014. Antibiotic-loaded silica nanoparticle–collagen composite hydrogels with prolonged antimicrobial activity for wound infection prevention. *J Mater Chem B* 2:4660–4670. <https://doi.org/10.1039/c4tb00327f>.
  26. Jiang B, Larson JC, Drapala PW, Pérez-Luna VH, Kang-Mieler JJ, Brey EM. 2012. Investigation of lysine acrylate containing poly (*N*-isopropylacrylamide) hydrogels as wound dressings in normal and infected wounds. *J Biomed Mater Res B Appl Biomater* 100:668–676. <https://doi.org/10.1002/jbm.b.31991>.
  27. Farnebo S, Woon CY, Schmitt T, Joubert L-M, Kim M, Pham H, Chang J. 2014. Design and characterization of an injectable tendon hydrogel: a novel scaffold for guided tissue regeneration in the musculoskeletal system. *Tissue Eng Part A* 20:1550–1561. <https://doi.org/10.1089/ten.TEA.2013.0207>.
  28. Browne S, Zeugolis DI, Pandit A. 2013. Collagen: finding a solution for the source. *Tissue Eng Part A* 19:1491–1494. <https://doi.org/10.1089/ten.TEA.2012.0721>.
  29. Shoseyov O, Posen Y, Grynspan F. 2014. Human collagen produced in plants: more than just another molecule. *Bioengineered* 5:49–52. <https://doi.org/10.4161/bioe.26002>.
  30. Williams TLD, Kaizawa Y. 2018. Collagen-based hydrogel accelerates wound healing in diabetic rats. 63rd Annual meeting, Plastic Surgery Research Council, 17 to 20 May 2018, Birmingham, AL.
  31. Jones V, Grey JE, Harding KG. 2006. Wound dressings. *BMJ* 332:777–780. <https://doi.org/10.1136/bmj.332.7544.777>.
  32. Khansa I, Schoenbrunner AR, Kraft CT, Janis JE. 2019. Silver in wound care—friend or foe?: a comprehensive review. *Plast Reconstr Surg Glob Open* 7:e2390. <https://doi.org/10.1097/GOX.0000000000002390>.
  33. Gould LJ. 2016. Topical collagen-based biomaterials for chronic wounds: rationale and clinical application. *Adv Wound Care (New Rochelle)* 5:19–31. <https://doi.org/10.1089/wound.2014.0595>.
  34. Naahidi S, Jafari M, Logan M, Wang Y, Yuan Y, Bae H, Dixon B, Chen P. 2017. Biocompatibility of hydrogel-based scaffolds for tissue engineering applications. *Biotechnol Adv* 35:530–544. <https://doi.org/10.1016/j.biotechadv.2017.05.006>.
  35. Kaizawa Y, Franklin A, Leyden J, Behn AW, Tulu US, Sotelo Leon D, Wang Z, Abrams GD, Chang J, Fox PM. 2019. Augmentation of chronic rotator cuff healing using adipose-derived stem cell-seeded human tendon-derived hydrogel. *J Orthop Res* 37:877–886. <https://doi.org/10.1002/jor.24250>.
  36. Kaizawa Y, Leyden J, Behn AW, Tulu US, Franklin A, Wang Z, Abrams G, Chang J, Fox PM. 2019. Human tendon-derived collagen hydrogel significantly improves biomechanical properties of the tendon-bone interface in a chronic rotator cuff injury model. *J Hand Surg* 44:899.e1–899.e11. <https://doi.org/10.1016/j.jhsa.2018.11.021>.
  37. Center for Disease Control and Prevention. 2017. Antibiotic resistance questions and answers. <https://www.cdc.gov/antibiotic-use/community/about/antibiotic-resistance-faqs.html>. Accessed 20 September 2018.
  38. Kirketerp-Møller K, Jensen PØ, Fazli M, Madsen KG, Pedersen J, Moser C, Tolker-Nielsen T, Høiby N, Givskov M, Bjarnsholt T. 2008. Distribution, organization, and ecology of bacteria in chronic wounds. *J Clin Microbiol* 46:2717–2722. <https://doi.org/10.1128/JCM.00501-08>.
  39. Wallace DG, Rosenblatt J. 2003. Collagen gel systems for sustained delivery and tissue engineering. *Adv Drug Deliv Rev* 55:1631–1649. <https://doi.org/10.1016/j.addr.2003.08.004>.
  40. Fonder MA, Lazarus GS, Cowan DA, Aronson-Cook B, Kohli AR, Mamelak AJ. 2008. Treating the chronic wound: a practical approach to the care of nonhealing wounds and wound care dressings. *J Am Acad Dermatol* 58:185–206. <https://doi.org/10.1016/j.jaad.2007.08.048>.
  41. Gonçalves C, Pereira P, Gama M. 2010. Self-assembled hydrogel nanoparticles for drug delivery applications. *Materials* 3:1420–1460. <https://doi.org/10.3390/ma3021420>.
  42. Serra R, Grande R, Butrico L, Rossi A, Settimio UF, Caroleo B, Amato B, Gallelli L, de Francis S. 2015. Chronic wound infections: the role of *Pseudomonas aeruginosa* and *Staphylococcus aureus*. *Expert Rev Anti Infect Ther* 13:605–613. <https://doi.org/10.1586/14787210.2015.1023291>.
  43. Yang L, Liu Y, Wu H, Høiby N, Molin S, Song Z. 2011. Current understanding of multi-species biofilms. *Int J Oral Sci* 3:74–81. <https://doi.org/10.4248/IJOS11027>.
  44. Bjarnsholt T, Alhede M, Alhede M, Eickhardt-Sørensen SR, Moser C, Kühl M, Jensen PØ, Høiby N. 2013. The *in vivo* biofilm. *Trends Microbiol* 21:466–474. <https://doi.org/10.1016/j.tim.2013.06.002>.
  45. Frutos P, Torrado S, Perez-Lorenzo M, Frutos G. 2000. A validated quantitative colorimetric assay for gentamicin. *J Pharm Biomed Anal* 21:1149–1159. [https://doi.org/10.1016/s0731-7085\(99\)00192-2](https://doi.org/10.1016/s0731-7085(99)00192-2).
  46. Ismail AFH, Mohamed F, Rosli LMM, Shafri MAM, Haris MS, Adina AB. 2016. Spectrophotometric determination of gentamicin loaded PLGA microparticles and method validation via ninhydrin-gentamicin complex as a rapid quantification approach. *J App Pharm Sci* 6:7–14. <https://doi.org/10.7324/JAPS.2016.600102>.
  47. Clinical and Laboratory Standards Institute. 2019. CLSI M100-ED29:2019. Performance standards for antimicrobial susceptibility testing, 29th ed. Clinical and Laboratory Standards Institute, Wayne, PA.
  48. Aiken SS, Cooper JJ, Florance H, Robinson MT, Michell S. 2015. Local release of antibiotics for surgical site infection management using high-purity calcium sulfate: an *in vitro* elution study. *Surg Infect (Larchmt)* 16:54–61. <https://doi.org/10.1089/sur.2013.162>.
  49. Zhao G, Hochwalt PC, Usui ML, Underwood RA, Singh PK, James GA, Stewart PS, Fleckman P, Olerud JE. 2010. Delayed wound healing in diabetic (db/db) mice with *Pseudomonas aeruginosa* biofilm challenge: a model for the study of chronic wounds. *Wound Repair Regen* 18:467–477. <https://doi.org/10.1111/j.1524-475X.2010.00608.x>.
  50. O'Toole GA. 2011. Microtiter dish biofilm formation assay. *J Vis Exp* 47:e2437. <https://doi.org/10.3791/2437>.